JAERI-M
82-003

THE CHARACTERISTICS OF CROSS FLOW IN A ROD BUNDLE

March 1982

Masahiro OSAKABE and Hiromichi ADACHI

日 本 原 子 力 研 究 所
Japan Atomic Energy Research Institute

JAERI-Mレポートは，日本原子力研究所が不定期に公刊している研究報告書です。
入手の問合わせは，日本原子力研究所技術情報部情報資料課（〒319-11茨城県那珂郡東海村）あて，お申しこしください。なお，このほかに財団法人原子力弘済会資料センター（〒319-11 茨城県那珂郡東海村日本原子力研究所内）で複写による実費頒布をおこなっております。

JAERI-M reports are issued irregularly.
Inquiries about availability of the reports should be addressed to Information ection Division of Technical Information, Japan Atomic Energy Research Institute, Tokai-mura, Naka-gun Ibaraki-ken 319-11, Japan.

編集兼発行　日本原子力研究所
印　　刷　(株)原子力資料サービス

JAERI-M 82-003

The Characteristics of Cross Flow in a Rod Bundle

Masahiro OSAKABE and Hiromichi ADACHI

Division of Reactor Safety,
Tokai Research Establishment, JAERI

(Received January 29, 1982)

Recently two-dimensional two-phase flow in the core of a light water reactor (LWR) has been receiving more attention especially in respect to the loss of coolant accident (LOCA). In this accident the two-phase cross flow occurs between the subchannels in the rod bundle. In analysis of this penomenon, the pressure loss of cross flow passing through the rod bundle is one of the important factors. An air/water loop operated at the atomospheric pressure was designed and constructed in an initial attempt to characterize the two-phase cross flow. The single-phase flow and the two-phase flow passing through the rod bundle with an attack angle ϕ against the axes of rods was studied. The pressure for the three different attack angles was measured. The single-phase pressure loss was compared with the same type model as that used in the COBRA-IV Code and the two-phase differential pressure was compared with the homogeneous and the drift flux models.

Keywords: Two-dimensional, LWR, LOCA, Cross-flow, Air/Water, Attack Angle, Rod, Bundle, COBRA, Model, Two Phase Flow, Comparative Evaluations

JAERI－M　82－003

模擬燃料集合体内横流れ特性

日本原子力研究所　東海研究所　安全工学部
刑部真弘・安達公道

（1982年1月29日受理）

近年，特に冷却材喪失事故(LOCA)に関連して，軽水型原子炉(LWR)の炉心における，二次元二相流が注目されてきた。この事故において，横流れ二相流が，燃料集合体サブチャンネル間に発生すると考えられている。この現象の解析にあたっては，燃料集合体内を通過する横流れの圧力損失が重要な因子の一つとなる。このため，横流れ二相流研究の最初の試みとして，水－空気二相流ループを製作し，これを用いて，ロッドの軸に対し，角度φの流れ方向をもつ単相および二相流の圧力損失特性を，三通りの角度φに対して調べた。単相での圧力損失は，COBRA－Ⅳコードに使用されているものと，同じ型の計算モデルと比較した。また二相の流れ方向圧力差は，均質流モデルとドリフトフラックスモデルの予測値と比較した。

Contents

目　　次

1. Introduction

Many investigations have been conducted on the flow in the rod bundle. Most of them have been devoted to the flow which is parallel or perpendicular to the rods.

Recently three-dimensional flow in the Light Water Nuclear Reactors (LWRs) has been receiving more attention especially in respect to Loss of Coolant Accident (LOCA). In this accident the cross-flow mixing of two-phases occurs between the subchannels in the rod bundle. This flow gives a two or three-dimensional effects to the total thermo-hydrodynamic phenomena. In analysing this effects, the pressure loss of the cross-flow passing through the rod bundle is one of the important factors.

An air/water loop operated at the atmospheric pressure was designed and constructed in an initial attempt to characterize the cross-flow. In this paper cross-flow is defined as the flow passing through the rod bundle and having an attack angle ϕ with the axes of rods. Three different rod bundles were installed in the section. Each bundle had a different attack angle between the flow and rod axis; ϕ = 30, 15, 0 degrees. An attack angle of 0 degrees means the flow is parallel to the rod axis.

First, the flow directional differential pressures for single-phase air flow were measured. The pressure loss at the different attack angles was investigated. And it was compared with the model used in the three-dimensional flow analysis code, COBRA-IV[1], which could simulate the effect of attack angle. Second, the flow -directional differential pressures for two-phase cross-flow were measured with the special condition with a constant cross-flow quality. The measured pressure difference, which consisted of static pressure differences and two-phase pressure losses, were compared with the homogeneous and the drift flux two-phase flow models. It was found that the flow could be treated by the homogeneous model at the attack angle ϕ = 30 degrees. As the attack angle became smaller, the flow could not be treated as homogeneous. At ϕ = 0 degrees the flow could be described by the drift flux model in this experiment.

2. Experimental apparatus and procedure

A schematic diagram of the test facility is shown in the Fig. 1. The stainless steel frame of test-section can be inclined θ degrees against the direction of the gravity force.

Water and Air were supplied to the test section after each flow rate was measured by a set of the rotor meters. Each set of rotor meters consists of three meters with different measuring ranges. The maximum water flow rates are 100 ℓ/min, 10 ℓ/min and 1 ℓ/min. The maximum Air flow rates are 10,000 ℓ/min, 1,000 ℓ/min and 100 ℓ/min respectively.

The front and rear walls of test section and rods are made of transparent acrylic resion. The diameter of rods was 10.7 mm. Rod bundle is in a square arrangement with a pitch of 14.3 mm. The rod diameter and the arrangement are the same as an actual PWR fuel bundle. Three types of rod bundles with different attack angles against the rod axis were installed in the test section.

The flow-directional differential pressures ΔP (See Fig. 1) were measured by pressure taps located on the front and rear walls. For the single-phase air flow, the differential pressure is measured by a Göttingen type manometer (the minimum measuring range is 1/20 mm H_2O). The differential pressures are measured between the span 400.4 mm at ϕ = 30 degrees, 663 mm at ϕ = 15 degrees, 600 mm at ϕ = 0 degrees. In the case of air/water two-phase flow, a differential pressure cell (D.P. cell) is used for measuring. The measured spans are 400.4 mm at ϕ = 30 degrees, 331.5 mm at ϕ = 15 degrees, 300 mm at ϕ = 0 degrees. The raw data with osillatory components of pressure difference from the D.P. cell were time-averaged.

3. Pressure loss of single-phase air flow

The pressure loss coefficient C_D and Reynolds number, Re, are defined as follows[2].

$$C_D = \frac{1}{2} \cdot \Delta P/(\rho V^2 N_T) \quad (\phi \neq 0 \text{ deg.}) \tag{1}$$

$$C_D = \frac{1}{2} \cdot \Delta P/(\rho V^2 \frac{R}{D_e}) \quad (\phi = 0 \text{ deg.}) \tag{2}$$

2. Experimental apparatus and procedure

A schematic diagram of the test facility is shown in the Fig. 1. The stainless steel frame of test-section can be inclined θ degrees against the direction of the gravity force.

Water and Air were supplied to the test section after each flow rate was measured by a set of the rotor meters. Each set of rotor meters consists of three meters with different measuring ranges. The maximum water flow rates are 100 ℓ/min, 10 ℓ/min and 1 ℓ/min. The maximum Air flow rates are 10,000 ℓ/min, 1,000 ℓ/min and 100 ℓ/min respectively.

The front and rear walls of test section and rods are made of transparent acrylic resion. The diameter of rods was 10.7 mm. Rod bundle is in a square arrangement with a pitch of 14.3 mm. The rod diameter and the arrangement are the same as an actual PWR fuel bundle. Three types of rod bundles with different attack angles against the rod axis were installed in the test section.

The flow-directional differential pressures ΔP (See Fig. 1) were measured by pressure taps located on the front and rear walls. For the single-phase air flow, the differential pressure is measured by a Göttingen type manometer (the minimum measuring range is 1/20 mm H_2O). The differential pressures are measured between the span 400.4 mm at ϕ = 30 degrees, 663 mm at ϕ = 15 degrees, 600 mm at ϕ = 0 degrees. In the case of air/water two-phase flow, a differential pressure cell (D.P. cell) is used for measuring. The measured spans are 400.4 mm at ϕ = 30 degrees, 331.5 mm at ϕ = 15 degrees, 300 mm at ϕ = 0 degrees. The raw data with osillatory components of pressure difference from the D.P. cell were time-averaged.

3. Pressure loss of single-phase air flow

The pressure loss coefficient C_D and Reynolds number, Re, are defined as follows[2].

$$C_D = \frac{1}{2} \cdot \Delta P/(\rho V^2 N_T) \quad (\phi \neq 0 \text{ deg.}) \tag{1}$$

$$C_D = \frac{1}{2} \cdot \Delta P/(\rho V^2 \frac{R}{D_e}) \quad (\phi = 0 \text{ deg.}) \tag{2}$$

$$R_e = V \cdot D/\nu \tag{3}$$

where N_T is the number of rows which the flow crosses. The Cross-section of the rows of rods in the flow direction are shown in Fig. 2. V is the velocity of the maximum free cross-section. The maximum free cross-section is defined as

89.4 mm (maximum free length in Fig. 2)
× 312 mm (width of test channel shown in Fig. 6).

As seen in the flow-directional cross-section in Fig..2, repeated cconvergent and divergent losses of the flow are imposed by the rods inlined 30 and 15 degrees against the flow-direction. When the pressure loss is mainly due to the expansion loss, the decrease of the attack angle ϕ results in a decrease of the expansion angle. The decrease of expansion angle means the elliptical cross-section of rod in Fig. 2 becomes elongated. So the pressure loss per one row of rod cross-sections becomes smaller as the attack angle ϕ decreases. This tendency can be seen on the test results at the higher Re number shown in Fig. 3. In Fig. 3 the pressure loss coefficients are shown. V in Eq.(3) for the ϕ = 0 degrees is also defined with the same free cross-section (89.4 mm × 312 mm). For the comparison at ϕ = 0 degrees, the correlations of laminar flow and Blasius type flow are shown in the Fig. 3.

Shown in Fig. 4 is the effect of attack angle on the pressure loss. The referred line are as follows. In the three-dimensional analysis code COBRA-IV, the flow in the rod bundle is divided to two spatial directions, parallel and normal to the rods. The following pressure loss coefficient C_D is used for the flow normal to the rods.

$$C_D = 1.57 \tag{4}$$

This pressure loss coefficient is defined as Eq.(1). This value agrees well with the experimental result[3] in the range of Re = $6 \times 10^2 \sim 6 \times 10^3$. The present results shown in Fig. 3 is available for the flow parallel to the rods.

$$C_D = 0.704\ Re^{-0.395} \tag{5}$$

When the flow is inclined ϕ degrees to the rods, the pressure loss ΔP_ϕ

can be expressed by the Eq.(4) and Eq.(5). The following simple equation is equivalent to the COBRA calculation if an infinite noding is used.

$$\Delta P_{\phi} = 4 \cdot 0.704 \, R_{eA}^{-0.395} \left(\frac{\rho V_A^2}{2}\right) \frac{R\cos\phi}{D_e} + 4 \cdot 1.57 \left(\frac{\rho V_T^2}{2}\right) \frac{R\sin\phi}{P} \qquad (6)$$

where $R_{eA} = v_A \cdot d/\nu$ $\qquad V_A = V\cos\phi$ $\qquad V_T = V\sin\phi$.

COBRA type calculation Eq.(6) and the experimental result are plotted in Fig. 4. The distance R is defined in Fig. 4 as 400.4 mm. COBRA-type calculation can describe well the effect of attack angle on the pressure loss in the experimental range of this paper as shown in Fig. 4.

The solid line of Zukauskas[3] in Fig. 4 is derived from his experimental result on heat transfer as follows. The friction loss is expressed with the assumption that the heat and momentum transport to the rod surface is analogous, as

$$(\Delta P_{\phi})_{friction} = \alpha_c \cdot \Delta P_{\phi=0 \text{ deg.}} \quad , \qquad (7)$$

where α_c is the increasing rate of heat transfer coefficient with the attack angle ϕ. The solid line in Fig. 4 are obtained from the Zukauskas' experimental data on heat transfer by using Eq.(7), suggesting that the divergent and convergent loss increases as the attack angle ϕ becomes larger. Because the momentum transport to the rod surface is the same as the wall friction loss. As the limiting case at ϕ = 90 degrees, the friction loss of a rod bundle consitutes only a small part of the total pressure loss as shown in the previous study.[3][4]

4. The characteristics of two-pahse cross-flow

The phase separation occurs when two-phase mixture passes through the inclined rod bundle at a low flow rate. Recently more attention has been paid to this phase-separation corresponding to the large scale two-phase flow experiments.[5] Also the phase separation is important in the two-phase cross-flow because it determines the quality of crossing flow. The quality of the two-phase flow is strongly related to the pressure loss. In this study the problem of phase-separation was

can be expressed by the Eq.(4) and Eq.(5). The following simple equation is equivalent to the COBRA calculation if an infinite noding is used.

$$\Delta P_\phi = 4 \cdot 0.704\ R_{eA}^{-0.395} \left(\frac{\rho V_A^2}{2}\right) \frac{R\cos\phi}{D_e} + 4 \cdot 1.57 \left(\frac{\rho V_T^2}{2}\right) \frac{R\sin\phi}{P} \qquad (6)$$

where $R_{eA} = v_A \cdot d/\nu$ $\qquad V_A = V\cos\phi$ $\qquad V_T = V\sin\phi$.

COBRA type calculation Eq.(6) and the experimental result are plotted in Fig. 4. The distance R is defined in Fig. 4 as 400.4 mm. COBRA-type calculation can describe well the effect of attack angle on the pressure loss in the experimental range of this paper as shown in Fig. 4.

The solid line of Zukauskas[3] in Fig. 4 is derived from his experimental result on heat transfer as follows. The friction loss is expressed with the assumption that the heat and momentum transport to the rod surface is analogous, as

$$(\Delta P_\phi)_{friction} = \alpha_c \cdot \Delta P_{\phi=0\ deg.} \ , \qquad (7)$$

where α_c is the increasing rate of heat transfer coefficient with the attack angle ϕ. The solid line in Fig. 4 are obtained from the Zukauskas' experimental data on heat transfer by using Eq.(7), suggesting that the divergent and convergent loss increases as the attack angle ϕ becomes larger. Because the momentum transport to the rod surface is the same as the wall friction loss. As the limiting case at ϕ = 90 degrees, the friction loss of a rod bundle consitutes only a small part of the total pressure loss as shown in the previous study.[3][4]

4. The characteristics of two-pahse cross-flow

The phase separation occurs when two-phase mixture passes through the inclined rod bundle at a low flow rate. Recently more attention has been paid to this phase-separation corresponding to the large scale two-phase flow experiments.[5] Also the phase separation is important in the two-phase cross-flow because it determines the quality of crossing flow. The quality of the two-phase flow is strongly related to the pressure loss. In this study the problem of phase-separation was

avoided as the first approach to the two-phase cross-flow. That was, the frame of test section was inclined 30 degrees to promote and saturate the phase separation. By this method the two-phase cross-flow of a constant quality could be investigated.

An example of the flow pattern is shown in Fig. 5. For simplicity, the flow-directional differential pressure was measured when the net flow rate of water from the test section was zero. The water was circulating in the test section. The differential pressure including the static pressure difference was measured.

It is important to compare the experimental data with some existing models in an initial attempt to characterize the two-phase cross flow. To investigate the characteristic of two-phase cross-flow the experimental result was compared with the homogeneous and drift flux models.

4.1 The model description

The parameters used in the present paper are defined in Fig. 6. ℓ_b is the mean width of two-phase part. The approximate two equations of the differential pressure are available in this flow pattern. Eq.(8) is the equation for the two-phase up-flow and Eq.(9) is for the single phase downflow.

$$\Delta P = \Delta P_{TF} + [\alpha\rho_g + (1-\alpha)\rho_f]g\ R\ \cos\theta \tag{8}$$

$$\Delta P = -\Delta P_f + \rho_f\ g\ R\ \cos\theta \tag{9}$$

where ΔP_{TF} and ΔP_f is the pressure loss for each flow. From Eq.(8) and Eq.(9)

$$\alpha(\rho_f - \rho_g)g\ R\ \cos\theta = \Delta P_{TF} + \Delta P_f \tag{10}$$

When the pressure loss coefficient defined in Eqs.(1) and (2) written as,

$$C_D = m\ R_e^{-n} \tag{11}$$

where m and n are constant. Then the single-phase pressure drop ΔP_f is described as,

$$\Delta P_f = C_f \, Q_f^{2-n} \quad . \tag{12}$$

where

$$C_f = \frac{1}{2^m}\left(\frac{D}{\nu_f}\right)^{-n} \left(\frac{1}{A_f}\right)^{2-n} \frac{R\sin\phi}{P} \rho_f \qquad (\phi \neq 0 \text{ deg.}) \tag{13}$$

$$C_f = \frac{1}{2^m}\left(\frac{D}{\nu_f}\right)^{-n} \left(\frac{1}{A_f}\right)^{2-n} \frac{R}{D_e} \rho_f \qquad (\phi = 0 \text{ deg.}) \tag{14}$$

A_f is the single-phase flow area defined later in Eq.(25).
Following models were adopted in this study for the two-phase pressure loss.

(1) Homogeneous model[6]

$$\Delta P_{TF} = \Phi_{LO} \cdot C_{TFf} \cdot \left[\frac{\rho_f Q_f + \rho_g Q_g}{\rho_f}\right]^{2-n} \tag{15}$$

where

$$\Phi_{LO} = \frac{\Delta P_{TF}}{\Delta P_{LO}} = \left[1 - \alpha + \alpha \left(\frac{\rho_g}{\rho_f}\right)\right]^{n-1} \tag{16}$$

$$C_{TFf} = \frac{1}{2^m} \left(\frac{D}{\nu_f}\right)^{-n} \left(\frac{1}{A_{TF}}\right)^{2-n} \frac{R\sin\phi}{P} \rho_f \qquad (\phi \neq 0 \text{ deg.}) \tag{17}$$

$$C_{TFf} = \frac{1}{2^m} \left(\frac{D}{\nu_f}\right)^{-n} \left(\frac{1}{A_{TF}}\right)^{2-n} \frac{R}{D_e} \rho_f \qquad (\phi = 0 \text{ deg.}) \tag{18}$$

A_{TF} is the two-phase flow area defined in Eq.(25). Eq.(15) is the correlation based on the single phase water flow. ΔP_{LO} is the pressure loss for the total flow within the channel flowing as if it had the physical properties of the water with the same mass flow. The correlation based on the single phase air flow is

$$\Delta P_{TF} = \Phi_{GO} \cdot C_{TFg} \cdot \left[\frac{\rho_f Q_f + \rho_g Q_g}{\rho_g}\right]^{2-n} \quad . \tag{19}$$

where

$$\Phi_{GO} = [1 + (1 - \alpha)\frac{\rho_f}{\rho_g}]^{-1} \tag{20}$$

$$C_{TFg} = \frac{1}{2}m \left(\frac{D}{\nu_g}\right)^{-n} \left(\frac{1}{A_{TF}}\right)^{2-n} \frac{R\sin\phi}{P} \rho_g \qquad (\phi \neq 0 \text{ deg.}) \tag{21}$$

$$C_{TFg} = \frac{1}{2}m \left(\frac{D}{\nu_g}\right)^{-n} \left(\frac{1}{A_{TF}}\right)^{2-n} \frac{R}{D_e} \rho_g \qquad (\phi = 0 \text{ deg.}) \tag{22}$$

Eq.(19) agrees closely with Diel's experiment[7] which was performed at ϕ = 90 degrees (staggered bank).

(2) Drift flux model[6],[8]

The drift flux model developed by Zuber is

$$(1-\alpha)Q_g - \alpha Q_f = 1.53\ \alpha \left[\frac{\sigma g \cos\theta (\rho_f - \rho_g)}{\rho_f^2}\right]^{1/4} A_{TFD} \ . \tag{23}$$

A_{TFD} is the two-phase flow area defined in Eqs.(26), (27). In Eq.(23), $\cos\theta$ is multiplied to the accelation constant of gravity, g, because the frame of test section is inclined θ degrees against the direction of gravity.

The following approximate two-fluid model description was used.

$$\Delta P_{TF} = C_{TFf} \left(\frac{Q_f}{1-\alpha}\right)^{2-n} + C_{TFg} \left(\frac{Q_g}{\alpha}\right)^{2-n} \tag{24}$$

C_{TFf} is defined by Eqs.(17) and (18). C_{TFg} is same as Eqs.(21) and (22). The pressure loss is due to the wall friction loss at the attack angle ϕ = 0 degrees. Then C_{TFg} should be set zero when the flow is bubbly or film flow regimes.[9] Similarly C_{TFf} should be zero for droplet flow (no film) or inverted annular flow. C_{TFg} was set zero in this study even at the attack angle $\phi \neq 0$.

To get the relation between Q_g and Q_f from the above equations, A_{TF} and A_f are needed. A_{TF} and A_f are defined as

$$\left.\begin{aligned} A_{TF} &= \ell_b \text{ mm (width of two-phase part in Fig. 6)} \\ &\quad \cdot 89.4 \text{ mm (maximum free length in Fig. 2)} \\ A_f &= \{312 \text{ mm (width of test channel shown in Fig.6)} - \ell_b \text{ mm}\} \\ &\quad \cdot 89.4 \text{ mm (maximum free length in Fig. 2)} \end{aligned}\right\} \tag{25}$$

where ℓ_b was measured and time-averaged. The value of ℓ_b is shown in Fig. 7. The experimental value shown in Fig. 7 was substituted in Eq.(25).

A_{TFD} in Eq.(23) in the cross-section where the drift flux is defined and this value is important to determine the void fraction. Two kinds of areas were used. One is maximum flow area

$$(A_{TFD})_{max.} = A_{TF} \quad . \tag{26}$$

The other is minimum flow area

$$(A_{TFD})_{min.} = \ell_b \cdot 25.2\text{mm (minimum free length in Fig. 2).} \tag{27}$$

The results in Fig. 3 were used for the constants, m and n. Because in this two-phase experiment, the corresponding Re of each phase is approximately within the same range.

4.2 Experimental result and comparison with the model

In this experimental condition, the flow pattern was bubbly or churn turbulent flow. The superficial velocity j_g at the two-phase up-flow was as follows in the range of $Q_g = 5 \times 10^3 \sim 7 \times 10^4$ cm^3/s.

1)	ϕ = 0 degrees	$j_g = 0.75 \sim 4.63$ m/s
2)	ϕ = 15, 30 degrees	$j_{g\ max.} = 1.67 \sim 10.3$ m/s
		$j_{g\ min.} = 0.42 \sim 2.6$ m/s

At ϕ = 15, 30 degrees, $j_{g\ max.}$ was defined at the minium flow area $(A_{TFD})_{min.}$ and $j_{g\ min.}$ was defined at the maximum flow area $(A_{TFD})_{max.}$ shown as Eqs.(26) and (27). The calculated superficial water velocity j_f at the two-phase up-flow defined at $(A_{TFD})_{min.}$ and $(A_{TFD})_{max.}$ was $0.2 \leq j_f \leq 1.3$ m/s for the calculations using the homogeneous and drift flux model at ϕ = 0, 15 and 30 degrees.

The differential pressure per unit flow-directional length is shown in Figs. 8, 9, 10. This pressure difference includes the static pressure drop which depends on the void fraction.

In the case of ϕ = 30 deg., experimental data agree closely with the homogeneous model. This is consistent with Diehl's experiment[7]

and Finlay's experiment[10] (ϕ = 90 deg., staggered bank). Their data agree well with the homogeneous model. Especially Diehl's data agree closely in the range of $\frac{Q_f}{Q_f + Q_g}\frac{\rho_f}{\rho_g} = 10^{-1} \sim 10^{2}$. At ϕ = 15 deg., the experimental data falls between the homogeneous model and the drift flux model. This is considered to be the transition region. At ϕ = 0 deg., experimental data fall on the predicted line of drift flux model presented by Eq.(23) and Eq.(24). In this way, at large attack angle ϕ, the flow can be treated as homogeneous flow for the repeated convergence and divergence. Smaller the attack angle ϕ degrees, the pressure loss begins to depend on the wall friction and the slip between two phase becomes larger. At the final stage ϕ = 0 degrees, it can be treated by the drift flux model.

In the model of COBRA-IV, two-phase flow can be treated by the drift flux or slip model in the direction parallel to the rods and by the homogeneous model in the direction normal to the rods. Then the COBRA-type calculation can be considered as an interpolation between the homogeneous model (ϕ = 90 deg.) and drift flux model (ϕ = 0 deg.) for the two-phase flow when the rods are inclined ϕ degrees. The tendency to change from the homogeneous model to the drift flux model is seen also in this experiment.

In this paper the characteristics of cross-flow without the phase-separation were investigated. In the future the characteristics of the phase-separation must be investigated. The actual cross-flow would be the complex phenomena with phase separation.

5. Conclusion

1. Single phase differential pressure with attack angle ϕ was investigated for the range of ϕ = 0 $\sim$ 30 degrees. It can be considered that the divergent and convergent pressure loss becomes smaller as the attack angle ϕ decreases. At ϕ = 0 degrees, the pressure loss is due to the wall friction only.
2. The characteristics of two-phase cross-flow were investigated. When the attack angle ϕ is 30 degrees, the flow can be treated as homogeneous. As the attack angle becomes smaller, the flow becomes not able to be treated as homogeneous. As the limiting

and Finlay's experiment[10] (ϕ = 90 deg., staggered bank). Their data agree well with the homogeneous model. Especially Diehl's data agree closely in the range of $\frac{Q_f}{Q_f + Q_g}\frac{\rho_f}{\rho_g} = 10^{-1} \sim 10^{2}$. At ϕ = 15 deg., the experimental data falls between the homogeneous model and the drift flux model. This is considered to be the transition region. At ϕ = 0 deg., experimental data fall on the predicted line of drift flux model presented by Eq.(23) and Eq.(24). In this way, at large attack angle ϕ, the flow can be treated as homogeneous flow for the repeated convergence and divergence. Smaller the attack angle ϕ degrees, the pressure loss begins to depend on the wall friction and the slip between two phase becomes larger. At the final stage ϕ = 0 degrees, it can be treated by the drift flux model.

In the model of COBRA-IV, two-phase flow can be treated by the drift flux or slip model in the direction parallel to the rods and by the homogeneous model in the direction normal to the rods. Then the COBRA-type calculation can be considered as an interpolation between the homogeneous model (ϕ = 90 deg.) and drift flux model (ϕ = 0 deg.) for the two-phase flow when the rods are inclined ϕ degrees. The tendency to change from the homogeneous model to the drift flux model is seen also in this experiment.

In this paper the characteristics of cross-flow without the phase-separation were investigated. In the future the characteristics of the phase-separation must be investigated. The actual cross-flow would be the complex phenomena with phase separation.

5. Conclusion

1. Single phase differential pressure with attack angle ϕ was investigated for the range of ϕ = 0 $\sim$ 30 degrees. It can be considered that the divergent and convergent pressure loss becomes smaller as the attack angle ϕ decreases. At ϕ = 0 degrees, the pressure loss is due to the wall friction only.
2. The characteristics of two-phase cross-flow were investigated. When the attack angle ϕ is 30 degrees, the flow can be treated as homogeneous. As the attack angle becomes smaller, the flow becomes not able to be treated as homogeneous. As the limiting

case, the flow can be treated with the drift flux model at ϕ = 0 deg.

Acknowledgement

The authors are much indebted to Dr. S. Katsuragi, Head of Div. Reactor Safety, Dr. M. Ishikawa, Deputy Head of Div. Reactor Safety and Dr. K. Hirano, Head of Reactor Safety Laboratory II, for their guidance and encouragement.

They would like to express their appreciation to Dr. Y. Sudo, Mr. A. Ohnuki and especially Mr. T. Iwamura for their useful discussions. They also would like to express their thanks to Mr. D.H. Miyasaki for his useful and hearty suggestions.

case, the flow can be treated with the drift flux model at ϕ = 0 deg.

Acknowledgement

The authors are much indebted to Dr. S. Katsuragi, Head of Div. Reactor Safety, Dr. M. Ishikawa, Deputy Head of Div. Reactor Safety and Dr. K. Hirano, Head of Reactor Safety Laboratory II, for their guidance and encouragement.

They would like to express their appreciation to Dr. Y. Sudo, Mr. A. Ohnuki and especially Mr. T. Iwamura for their useful discussions. They also would like to express their thanks to Mr. D.H. Miyasaki for his useful and hearty suggestions.

References

(1) Stewart, C.W., et al.: COBRA-IV, The model and the method, BNWL-2214, (1977).

(2) Knudsen, J.G. and Katz, D.L.: Fluid dynamics and heat transfer, McGraw-Hill (1958).

(3) ZuKauskas, A.: Advance in heat transfer, 93, Academic Press. (1972).

(4) Achenbach, E., Wärme stopfübertragung 2, 47 (1969).

(5) Barasch, M., Lahey, R.T.: The measurement of two-dimensional phase separation phenomena, NUREG/CR-1936, (1981).

(6) Wallis, G.B.: One-dimensional Two-phase flow, McGraw-Hill, (1969).

(7) Diehl, J.E. and Unruh, C.H.: Two-phase pressure drop for horizontal Cross-flow through tube banks, ASME paper 58-HT-20, (1958).

(8) Zuber, N. and Findlay, J.A.: J. Heat Transfer, VOl.87, Ser. C., P.453, (1965).

(9) Hewitt, G.F. and Hall-Taylor, N.S.: Annular Two-pahse flow, pergamon press. (1970).

(10) Finlay, I.C. and Mcmilan, T.: Pressure loss during Air/Water mist flow across a staggered bank of tubes, Int. J. Multiphase Flow, Vol.1, P.601, (1974).

Nomenclature

θ	:	The angle inclined against the gravity
ϕ	:	The attack angle to the rods
ΔP	:	Total flow-directional pressure difference
ΔP_{TF}	:	Pressure loss of two-phase part
ΔP_f	:	Pressure loss of water down flow
ρ	:	Density
N_T	:	Row number of rods crossed by the fluid
C_D	:	Pressure loss coefficient
P	:	Pitch (= 14.3 mm)
D	:	Rod diameter (= 10.7 mm)
D_e	:	Equivalent diameter of subchannel ($= 4 \cdot \frac{P^2 - \pi D^2/4}{\pi D}$)
R	::	Flow-directional distance
V	:	The velocity of maximum free cross-section
ν	:	Kinematic viscosity
σ	:	Surface tension
Re	:	Reynols number defined in Eq.(3)
Q	:	Volumetric flow rate
g	:	Gravitational accelation constant
α	:	Void fraction
A	:	Flow free cross section
ℓ_b	:	Width of two-phase part
m, n	:	Constants defined in Eq.(10)
A_{TF}, A_f	:	Defined in Eq.(25)
A_{TFD}	:	Defined in Eq.(26) and Eq.(27)

Subscript

g	:	Air
f	:	Water
TF	:	Two-phase

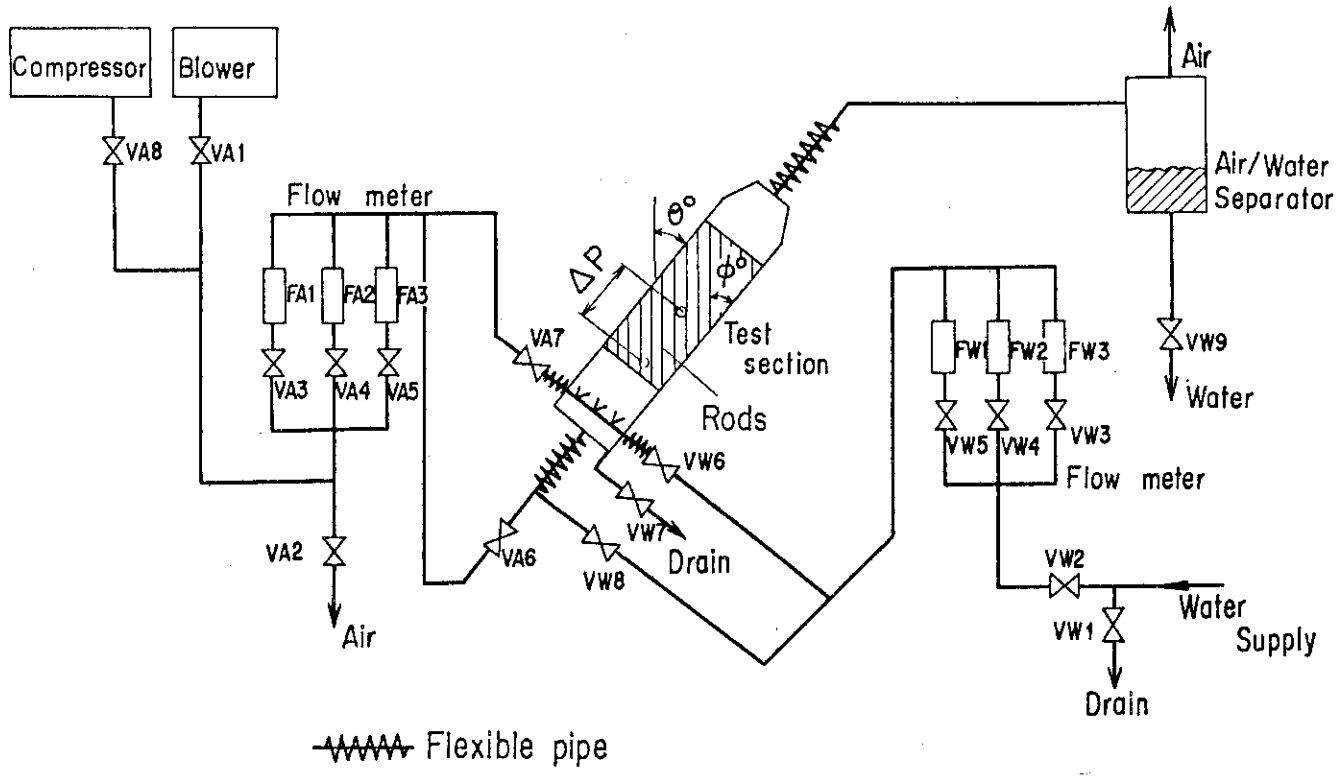

Fig 1: Scematic diagram of test facility.

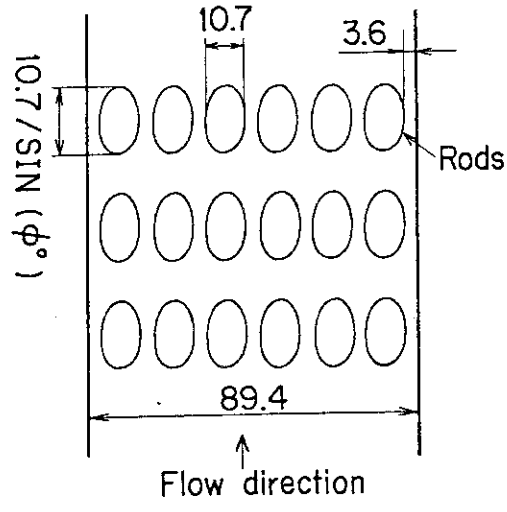

Fig 2: Flow directional cross-section.

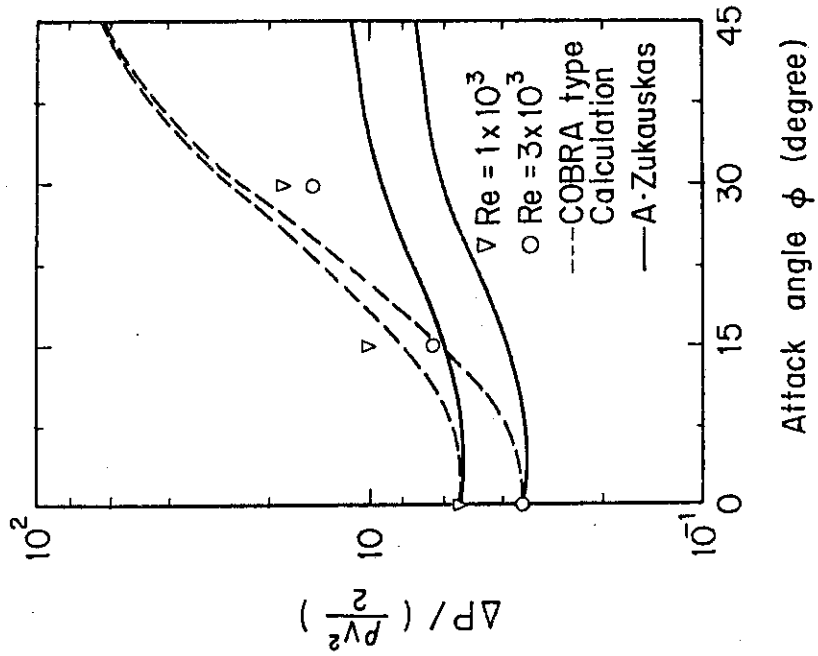

Fig 4: Effect of attack angle on the pressure loss.

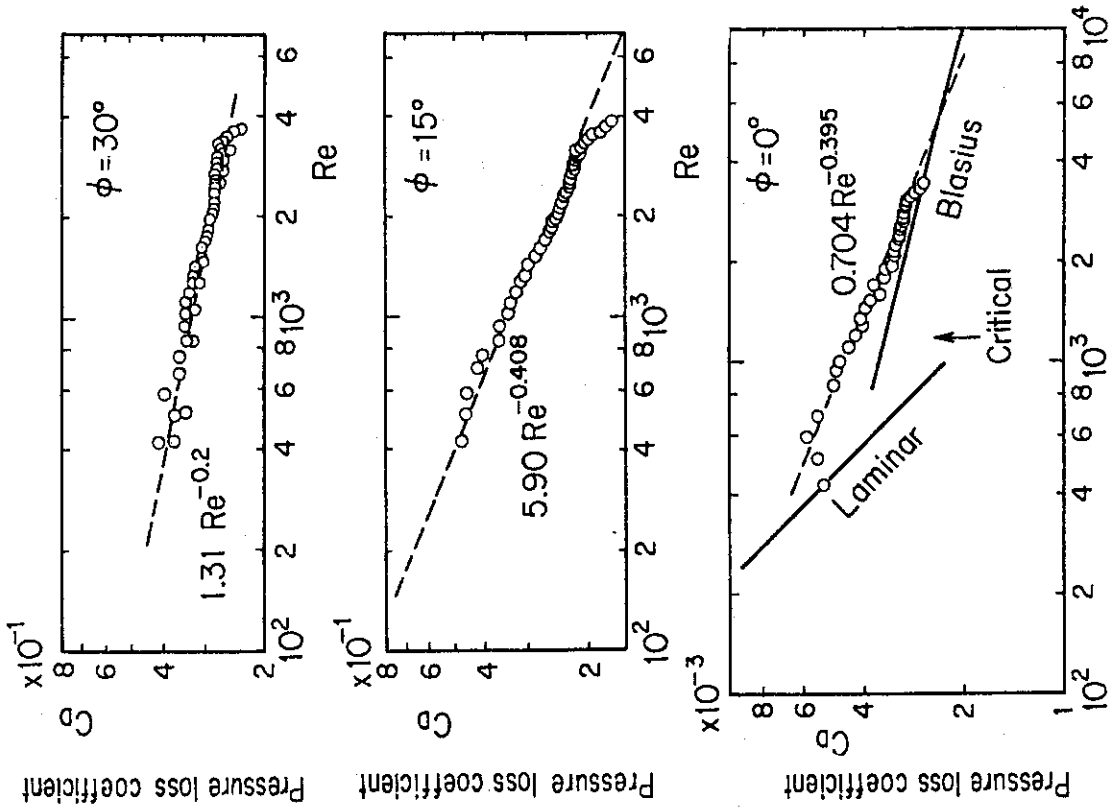

Fig 3: Pressure loss coefficient of the single-phase flow.

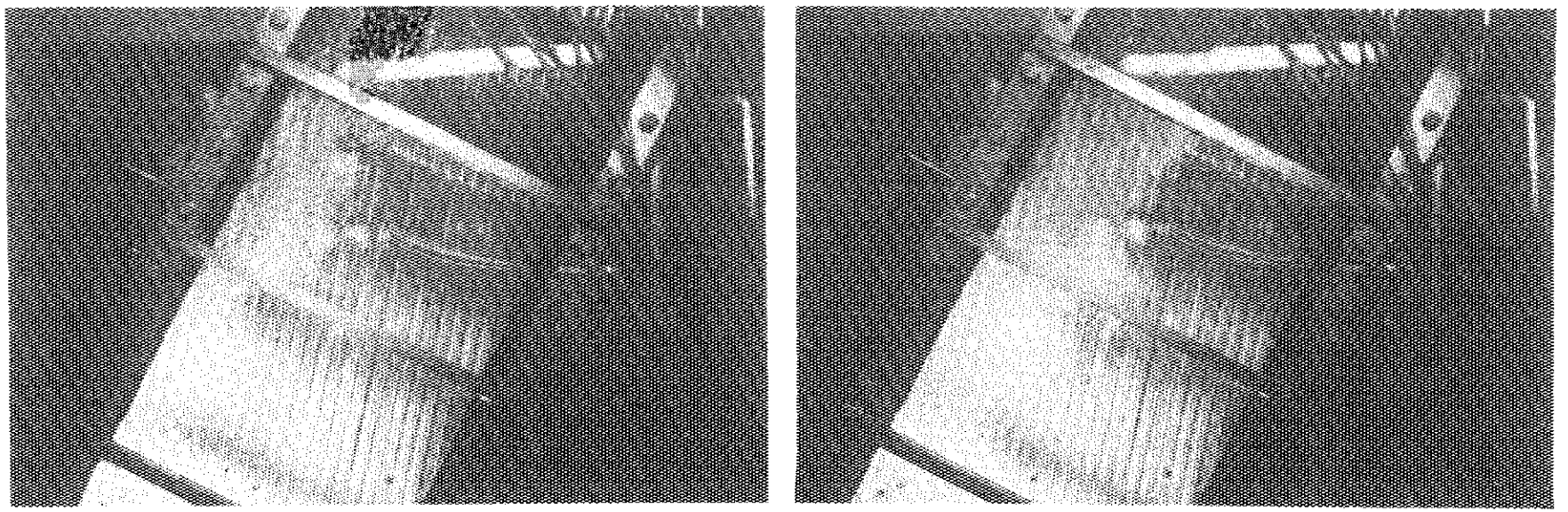

(1) ϕ = 15 degrees

$Q_g = 1.67 \times 10^3$ cm^3/s

$Q_l = 6.67 \times 10^2$ cm^3/s

(2) ϕ = 15 degrees

$Q_g = 6.67 \times 10^3$ cm^3/s

$Q_l = 1.67 \times 10^3$ cm^3/s

Fig 5: Photograph of the flow pattern.

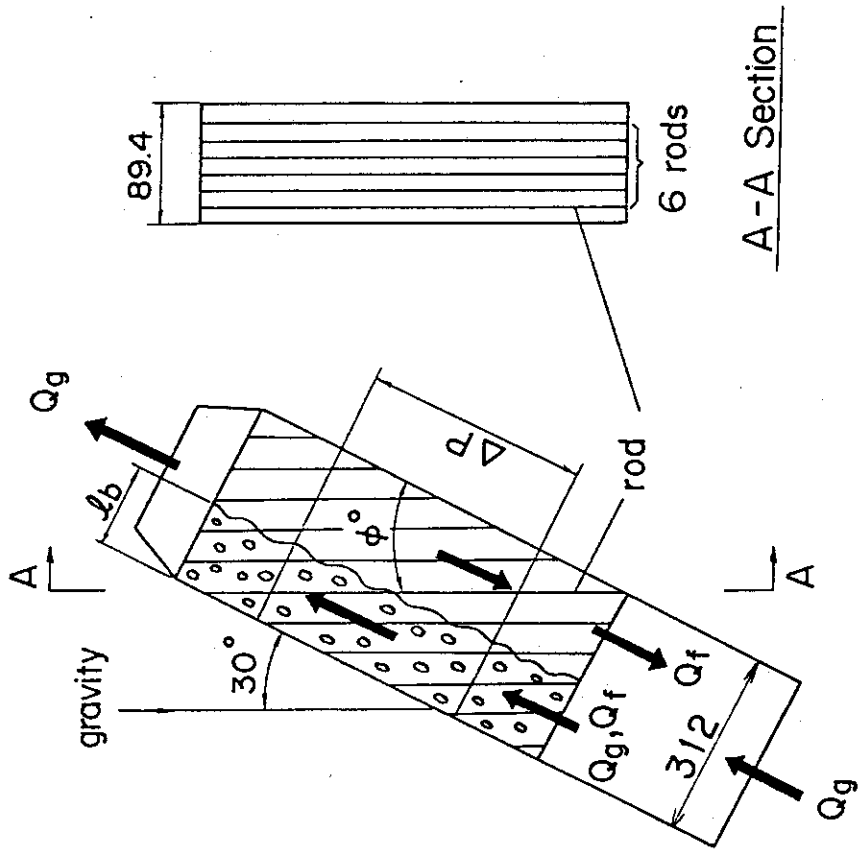

Fig 6: Two-phase flow experiment.

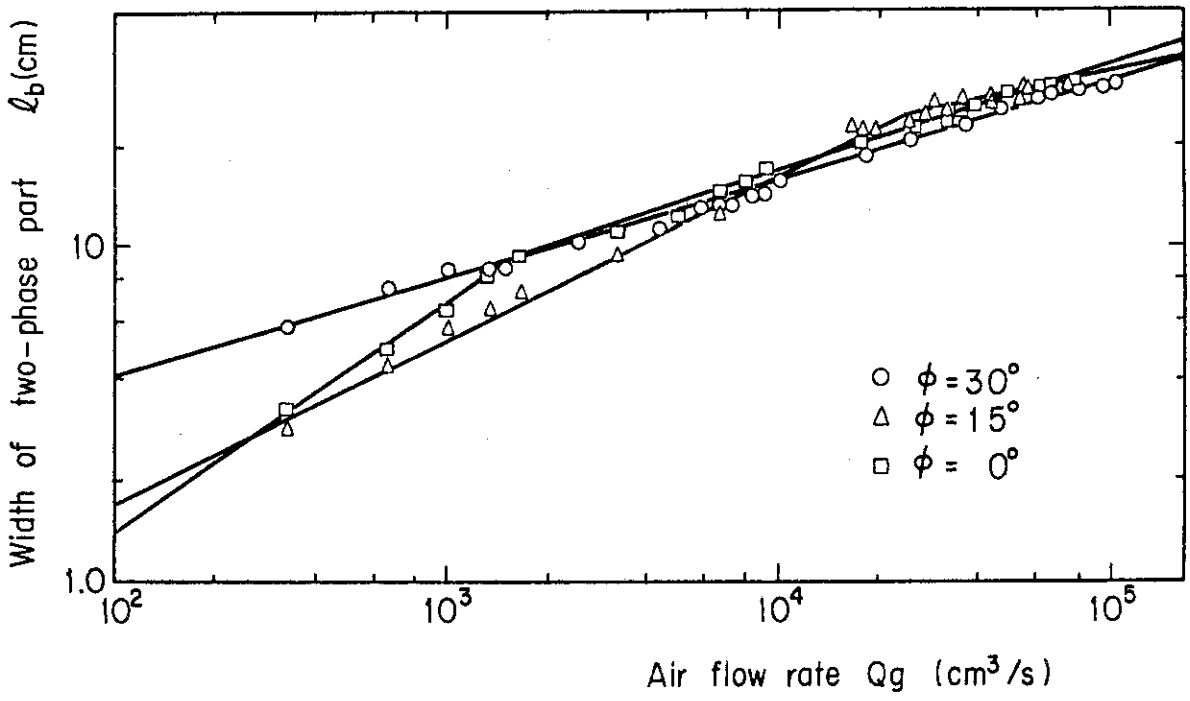

Fig 7: Width of the two-phase part.

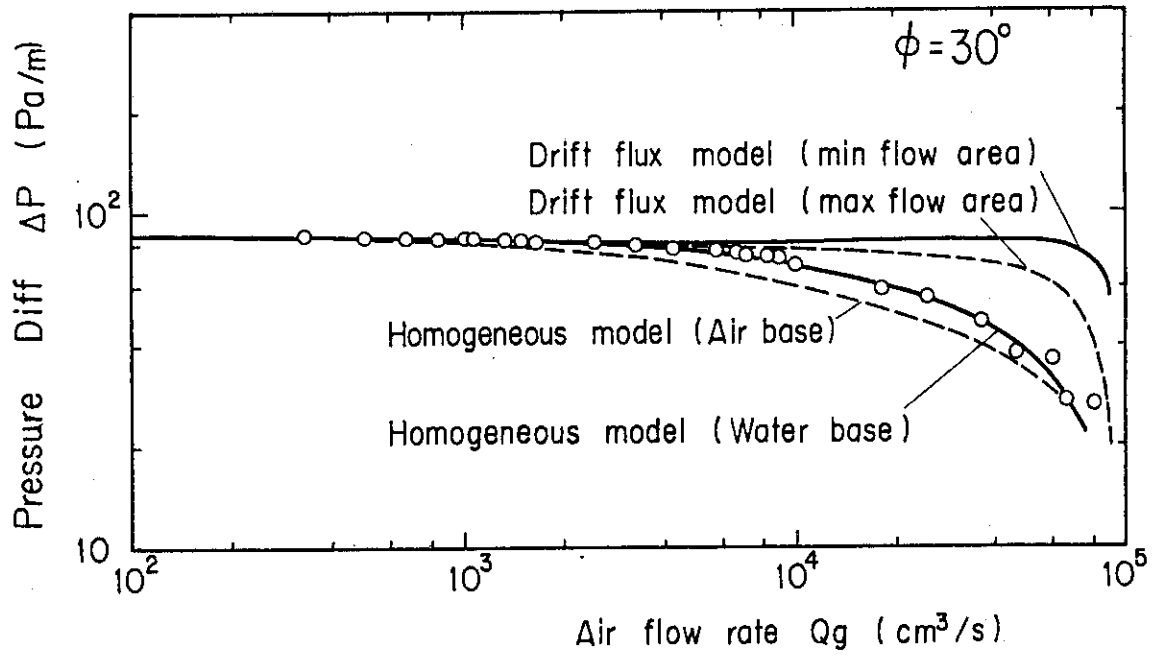

Fig 8: Differential pressure in the case of φ = 30 degrees.

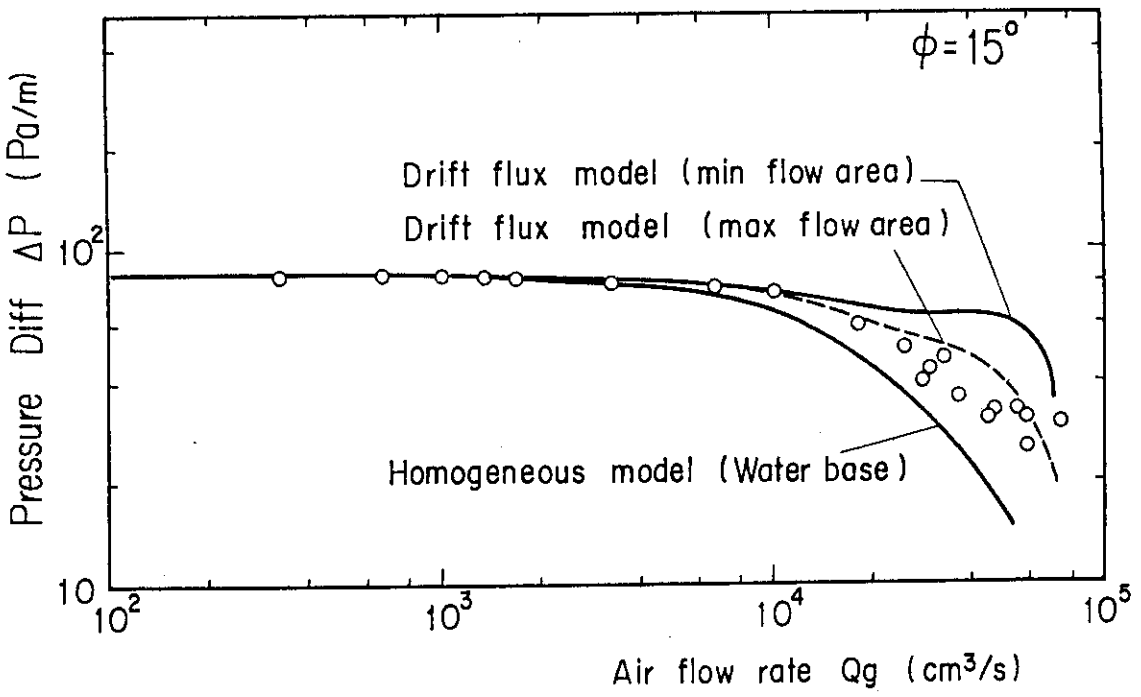

Fig 9: Differential pressure in the case of φ = 15 degrees.

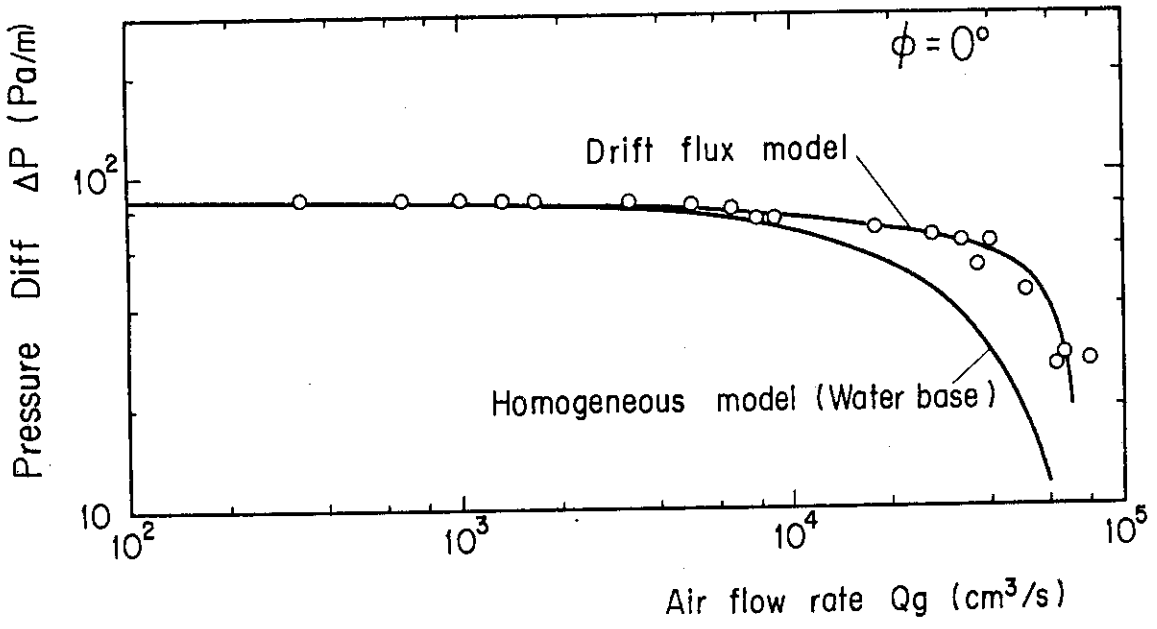

Fig 10: Differential pressure in the case of φ = 0 degrees.